Vertical boundary at $x \approx 0.11$ in the structural phase diagram of the La$_{1-x}$Sr$_x$MnO$_3$ system ($0.08 \leqslant x \leqslant 0.125$)

D. E. Cox, T. Iglesias,* and E. Moshopoulou†

Department of Physics, Brookhaven National Laboratory, Upton, New York 11973-5000

K. Hirota, K. Takahashi, and Y. Endoh‡

CREST, Department of Physics, Tohoku University, Sendai 980-8578, Japan
(Received 23 October 2000; published 22 June 2001)

The structural phase diagram of the La$_{1-x}$Sr$_x$MnO$_3$ system in the compositional range $0.08 \leqslant x \leqslant 0.125$ has been investigated by high-resolution synchrotron x-ray powder diffraction techniques between $20-600$ K. Recent studies have reported that there is an unusual reentrant-type phase transition in this range involving an abrupt change in lattice parameters but no change in the crystal symmetry, which remains orthorhombic *Pbnm*. The transition to the reentrant phase is from a ferromagnetic metallic to a ferromagnetic insulating phase with some unusual properties. Our results demonstrate that for samples with $x = 0.11 - 0.125$ there exist two lower-symmetry structural regions having monoclinic and triclinic symmetry, respectively. There is a sharp first-order transition from the monoclinic to the triclinic phase coinciding with the transition to the ferromagnetic insulating phase, and an abrupt crossover from the orthorhombic *Pbnm* region with a near-vertical phase boundary just below $x = 0.11$. The new phases indicate the presence of some novel type of orbital ordering unlike that found in LaMnO$_3$.

I. INTRODUCTION

Since the recent discovery of colossal magnetoresistance in doped rare-earth manganate perovskites of the type La$_{1-x}$A$_x$MnO$_3$ ($A = $ Ca,Sr,Ba),[1] there has been an enormous amount of attention focussed on the relationships among magnetic, electrical, and structural properties, especially with respect to the delicate and complex balance between charge, orbital, and magnetic ordering. Considerable progress has been made in understanding the physics of these materials, and it is now widely accepted that although the traditional double-exchange mechanism originally proposed by Zener[2–4] is qualitatively able to account for the ferromagnetic metallic (FMM) state observed at intermediate doping levels of $x \approx 0.2 - 0.4$,[5,6] it is not capable of explaining many of the other magnetic and transport properties.[7] Some important recent advances have been the recognition of the importance of electron-phonon coupling effects,[8,9] calculations which show a tendency for these materials towards phase separation,[10,11] and the application of x-ray resonant scattering techniques as a probe of orbital ordering.[12] In the case of LaMnO$_3$, such techniques have provided direct evidence of the orbital ordering of distorted MnO$_6$ octahedra associated with a cooperative Jahn-Teller (JT) effect previously inferred on the basis of bond distances obtained from structure determinations.

One of the important and intriguing remaining questions is the nature of the ferromagnetic insulating (FMI) phase in lightly doped La$_{1-x}$Sr$_x$MnO$_3$ with $x \approx 0.10 - 0.15$.[13] A usual feature of this phase is that neutron diffraction measurements have shown that for $x = 0.125$ there is first a transition to a FMM phase from the paramagnetic insulating (PMI) state at higher temperatures, followed by an abrupt first-order transition to the FMI phase,[14,15] accompanied by the appearance of

a weak antiferromagnetic component with the A-type magnetic structure similar to that found in LaMnO$_3$.[16] In another neutron diffraction study of crystals with $x = 0.10$ and 0.15, Yamada *et al.*[17] observed that the FMI phase gave weak superlattice peaks which they attributed to long-range ordering of Mn^{4+} ions over 1/8 of the Mn sites, and this type of charge-ordering scenario has been accepted in most subsequent publications in the literature. However, a recent neutron and synchrotron x-ray study of a crystal with $x = 0.12$ has demonstrated that conventional charge ordering does not occur, and that the key parameter in the transition to the FMI phase is the orbital degree of freedom of the e_g electrons.[18,19]

The present paper describes the results of a high-resolution synchrotron x-ray powder diffraction study carried out on several compositions in the range $x = 0.08 - 0.125$. The samples were obtained from fragments of crystals grown in exactly the same way as the one used by Endoh *et al.*[18] The results demonstrate the existence of two previously unreported lower-symmetry phases with monoclinic and triclinic symmetry respectively in this region of the phase diagram, separated by a sharp boundary at $x \approx 0.11$ from the JT-ordered LaMnO$_3$-type orthorhombic phase which exists at lower values of x.

II. STRUCTURAL CONSIDERATIONS

Before describing the results of the present study, we first review briefly some of the relevant structural literature. The room-temperature structure of the parent compound LaMnO$_3$ has been reported by several groups to have a distorted perovskitelike structure with orthorhombic *Pbnm* symmetry, and lattice parameters $a \approx \sqrt{2} \times a_0$, $b \approx \sqrt{2} \times a_0$, $c \approx 2 \times a_0$, where a_0 is the parameter of the ideal cubic lattice.[20–23] As described in a detailed neutron powder diffraction study by

Rodriguez-Carvajal *et al.*,[23] the structure has lattice parameters $a = 5.5367$, $b = 5.7473$, $c = 7.6929$ Å, and is characterized by an octahedral tilt arrangement of the type $a^-a^-c^+$ (Ref. 24) and antiferrodistortive orbital ordering in the ab plane associated with a cooperative JT effect, resulting in two long Mn-O bond distances of 2.18 Å and four shorter ones (2×1.91 and 2×1.97 Å). Because of the orbital ordering, the spontaneous orthorhombic strain s in the basal plane [defined as $s = 2(a-b)/(a+b)$] is unusually large (about -3.7%) in LaMnO$_3$ compared to that in most $Pbnm$-type perovskites, and the c axis is significantly shortened ($c/\sqrt{2} = 5.4397$ Å). The orbital ordering disappears at ~ 750 K, above which the lattice is metrically cubic. However, Rietveld refinements show that the octahedral tilt angle decreases very little through the transition, and the structure is still unequivocally orthorhombic. At ~ 1010 K there is a further transformation to a rhombohedral structure with $R\bar{3}c$ symmetry, but this $R\bar{3}c$ phase will not be of any concern in the present paper. The JT-ordered structure is usually designated O', and the ''pseudocubic'' disordered structure O or O^*. The latter notation will be used hereafter.

In contrast to the LaMnO$_3$ samples used in the other structural studies, which were prepared by conventional solid-state synthesis, the one used by Rodriguez-Carvajal *et al.*[23] was prepared by crushing single-crystal ingots grown by the floating-zone method. They emphasize that the structural properties are very sensitive to the amount of Mn^{4+} introduced during synthesis; for example, the spontaneous orthorhombic strain decreases, the c parameter increases, and the transition temperatures to the pseudocubic and rhombohedral phases decrease quite rapidly with increasing Mn^{4+} content.

The influence of oxygen partial pressure and the formation of Mn^{4+} during the synthesis of ceramic samples was earlier discussed by Mitchell *et al.*[25] in an investigation of the room-temperature structural phase diagram of La$_{1-x}$Sr$_x$MnO$_{3+\delta}$. For $x<0.125$, oxygen partial pressures $p(O_2)$ of $<10^{-2}$ are needed to stabilize the $Pbnm$ phase. These authors also report that LaMnO$_3$ prepared under a $p(O_2)$ of $<10^{-3}$ has a monoclinic structure with $P2_1/c$ symmetry, with lattice parameters and atomic positions very similar to those of the orthorhombic $Pbnm$ structure.[26]

The variation of room-temperature lattice parameters in single crystals of La$_{1-x}$Sr$_x$MnO$_3$ with increasing x is nicely illustrated in Fig. 1 of Urushibara *et al.*,[13] which shows a rapid decrease in spontaneous orthorhombic strain and an increase in $c/\sqrt{2}$ up to $x=0.1$, a pseusocubic cell at $x=0.15$, and a transition to the rhombohedral structure at $x=0.175$. The electronic phase diagram shows a narrow FMI region between $x \approx 0.10-0.15$ at temperatures below $\sim 150-200$ K. Subsequent neutron diffraction studies on samples with $x=0.125$ (Refs. 15,27,28) revealed a very unusual structural transition around 150 K from a JT-distorted O' phase to a pseudocubic structure metrically similar to that at 300 K and designated O^* by Kawano *et al.*,[15] who described this as a ''reentrant'' transition, and presented schematic structural and magnetic phase diagrams. A more detailed structural phase diagram was reported by Pinsard *et al.*,[29]
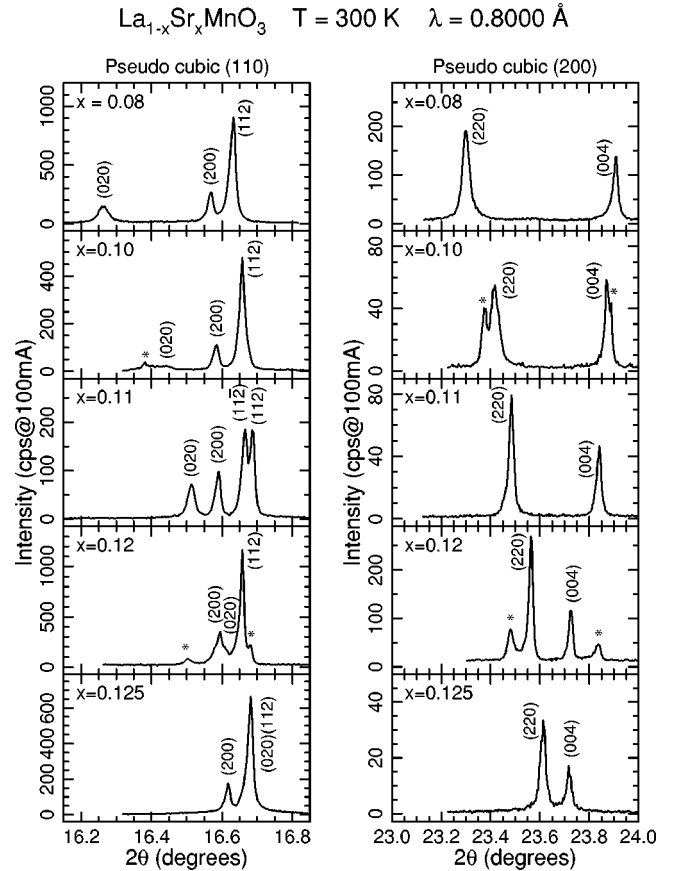

La$_{1-x}$Sr$_x$MnO$_3$ T = 300 K λ = 0.8000 Å

FIG. 1. Peak profiles of the pseudocubic (110) and (200) regions at 300 K for the five nominal compositions $x = 0.08, 0.10, 0.11, 0.12$, and 0.125. Peaks from the minority phases are indicated with asterisks. Note the splitting of the (112) reflection for $x = 0.11$.

who found the low-temperature reentrant phase existed only in the narrow range of composition $0.10 < x < 0.14$.

In the meantime, Yamada *et al.*[17] reported a neutron diffraction study of single crystals with $x = 0.10$ and 0.15, in which they noted the appearance of superlattice peaks in the FMI region which could be indexed in terms of a doubling of the orthorhombic c axis. They proposed a model structure consisting of alternating layers of Mn^{4+} ions ordered on 1/4 of the Mn sites interleaved with layers of orbitally ordered Mn^{3+} ions similar to those in LaMnO$_3$, but did not provide any quantitative intensity data in support of this model.

Similar superlattice peaks were observed in a high-energy synchrotron x-ray study of crystals with $x = 0.125$ and 0.15,[30] and in a recent neutron and synchrotron x-ray study of a crystal with $x = 0.12$.[18] A striking result of the latter study was that x-ray resonant scattering techniques revealed the existence of orbital ordering in the FMI region below 145 K. Although this behavior shows a resemblance to that reported for LaMnO$_3$,[12] there is a very significant difference, namely that a resonant signal was *not* observed in the JT-distorted region above the transition, but *only* in the pseudocubic reentrant region. Thus, the nature of the JT-type order in the intermediate region is clearly different from the $(d_{3x^2-r^2}/d_{3y^2-r^2})$-type orbital order in LaMnO$_3$. Further evidence for such a difference is provided by the spin-wave

dispersion measurements of Hirota *et al.*,[31] who found a dimensional ''crossover'' at around $x=0.1$ from the two-dimensional state in $LaMnO_3$ to a three-dimensional isotropic ferromagnetic state. Endoh *et al.*[18] also note that the superlattice peaks do not show the expected resonance features characteristic of charge-ordering. Thus although there is clearly some kind of structural modulation along the *c* axis, it cannot be attributed to conventional charge or orbital ordering. Furthermore, magnetization measurements show clearly that the low-temperature ferromagnetic phase is stabilized by the application of a magnetic field,[32–34] whereas a charge-ordered structure would be expected to melt in high magnetic fields. The experimental features of the transition are well accounted for by a theory in which the orbital degree of freedom is considered in the presence of strong electron correlations,[35] and Endoh *et al.*[18] conclude that it is this orbital degree of freedom which is the key parameter in the transition.

III. EXPERIMENTAL DETAILS

Single crystals of $La_{1-x}Sr_xMnO_3$ with nominal compositions $x=0.08, 0.10, 0.11, 0.12$, and 0.125 were grown in a floating-zone furnace. For subsequent powder diffraction studies, particular attention was given to the preparation of suitable samples in order to minimize possible broadening of the peak profiles due to induced microstrain or too small a particle size. Small fragments of the crystals were crushed and lightly ground in an agate mortar under acetone, and the fraction retained between $325-400$ mesh sieves ($\sim 38-44$ μm) was loaded into an 0.2 mm glass capillary which was then sealed. High-resolution synchrotron x-ray data were collected on several different occasions at beamline X7A at the Brookhaven National Synchrotron Light Source with a flat Ge(220) analyzer crystal, set for a wavelength between $0.7-0.8$ Å. With this diffraction geometry, the instrumental resolution over the 2θ range $5-30°$ is $0.005-0.01°$ full width at half maximum (FWHM), an order-of-magnitude better than that of a typical laboratory diffractometer. In some cases, extended data sets were obtained with a linear position-sensitive detector, which has the advantage of giving greatly improved counting statistics but with lower resolution (FWHM $\approx 0.03°$).

For low-temperature runs the capillary was mounted in a closed-cycle helium cryostat, and scans were made over selected angular regions with a step-size of typically $0.005°$. During each counting interval, the sample was rocked over several degrees, which is essential to achieve powder averaging over crystallites of this size. For runs above room temperature, the capillary was mounted in a wire-wound boron nitride tube furnace, and rotated continuously at about 1 Hz during data collection. Data were collected over regions corresponding to the pseudocubic (100), (110), (111), (200), (220), and (222) reflections, and also the orthorhombic (021) region on selected occasions. Least-squares fits to the observed peak profiles were made based on a pseudo-Voigt function with appropriate corrections for low-angle asymmetry due to axial divergence.[36] This procedure provides an accurate description of the peak shapes, which is crucial for

TABLE I. Indices of split peaks derived from a cubic perovskite cell with lattice parameter a_0 in a distorted cell with $a\approx\sqrt{2}\times a_0$, $b\approx\sqrt{2}\times a_0$, $c\approx 2\times a_0$, as the symmetry is successively lowered to orthorhombic, monoclinic and triclinic. The relative intensities within each group are approximately equal to the multiplicities of the powder reflections given in parentheses.

Cubic		Orthorhombic $(\alpha,\beta,\gamma=90°)$		Monoclinic $(\alpha\neq 90°)$		Triclinic $(\alpha,\beta,\gamma\neq 90°)$
						110 (2)
		110 (4)	−	110 (4)	<	
						$1\bar{1}0$ (2)
100 (6)	<					
		002 (2)	−	002 (2)	−	002 (2)
		200 (2)	−	200 (2)	−	200 (2)
		020 (2)	−	020 (2)	−	020 (2)
110						112 (12)
	<			112 (4)	<	
(12)						$1\bar{1}2$ (2)
		112 (8)	<			
						$11\bar{2}$ (2)
				$11\bar{2}$ (4)	<	
						$1\bar{1}\bar{2}$ (2)
						202 (2)
		202 (4)	−	202 (4)	<	
						$20\bar{2}$ (2)
111 (8)	<			022 (2)	−	022 (2)
		022 (4)	<			
				$02\bar{2}$ (2)	−	$02\bar{2}$ (2)

the identification of coexisting perovskitelike phases with low symmetry and similar lattice parameters.

The crystal symmetry of a distorted perovskitelike structure can be determined uniquely from the characteristic splitting of the pseudocubic $(h00)$, $(hh0)$, and (hhh) peaks. As mentioned above, the parent compound $LaMnO_3$ has orthorhombic *Pbnm* symmetry, with unit cell dimensions $a\approx\sqrt{2}\times a_0$, $b\approx\sqrt{2}\times a_0$, $c\approx 2\times a_0$, where a_0 is the edge of the simple cubic cell, and the split peaks have the indices and relative intensities listed in Table I. For lower crystal symmetries, additional splittings of some of the peaks occur, as will be described later. Another feature of the distorted *Pbnm* structure is the appearance of weak superlattice peaks resulting from a combination of octahedral tilts and shifts of the large *A*-site cations from the ideal cubic positions. The (021) superlattice peak is especially significant in this respect, since it provides the means to uniquely identify the *b* parameter [the corresponding (201) reflection being forbidden in *Pbnm* for symmetry reasons] and is well resolved from the adjacent fundamental reflections. It cannot be overemphasized that for the very small distortions observed in some of these materials, extremely high resolution is needed for a correct assignment of the crystal symmetry. The task is

TABLE II. Lattice parameters and unit cell volumes at 300 K for the majority and minority phases in $La_{1-x}Sr_xMnO_3$ with nominal compositions $x=0.08,0.10,0.11,0.12$, and 0.125. The ratios of the majority and minority phases were estimated from the relative intensities of the (220)/(004) pairs of reflections, and the x-ray compositions were derived from these ratios and the unit-cell volume as described in the text. The temperature of the $O^*-O'_{JT}$ transition was chosen to be where the sharpest decrease in the c lattice parameter occurred.

x	x (x ray)	Ratio	a (Å)	b (Å)	c (Å)	α (°)	Vol. (Å^3)	T_{O*O} (K)	T_{MT} (K)
0.08	0.079	80 %	5.5509	5.6549	7.7226	90.0	242.41	550	
	0.083	20 %	5.5510	5.6476	7.7280	90.0	242.27	530	
0.10	0.102	75 %	5.5469	5.6033	7.7362	90.0	240.45	435	
	0.095	25 %	5.5472	5.6212	7.7308	90.0	241.07	455	
0.11	0.110	95 %	5.5486	5.5743	7.7494	90.114	239.69	320	105
	0.107[a]	5 %	5.5457	5.5828	7.7541	90.0	240.07	>325	
0.12	0.122[b]	75 %	5.5421	5.5379	7.7842	90.0	238.91	295	140
	0.112[b]	25 %	5.5459	5.5734	7.7485	90.120	239.50	320	120
0.125	0.125	100 %	5.5437	5.5257	7.7929	90.0	238.72	280	140

[a]Estimated from lattice parameters at 325 K.
[b]Lattice parameters from interpolation between 295 and 305 K.

further complicated by the coexistence of two phases in most of the samples.

IV. RESULTS

Some representative scans at 300 K over the pseudocubic (110) and (200) regions are shown in Fig. 1 for the five compositions. It is clear from these scans that the samples with $x=0.10$ and 0.12 contain substantial amounts of a second phase with slightly different lattice parameters. Furthermore, a careful analysis of the pseudocubic (200) peak profiles reveals that there is also a second minority phase in the samples with $x=0.08$ and 0.11, and that only the $x=0.125$ sample can be considered to be single phase. However, the most striking feature in Fig. 1 is the splitting at the orthorhombic (112) position for $x=0.11$ into two roughly equal components, which is conclusive evidence of a lower symmetry (Table I). Analysis of the complete set of peak profiles for this material revealed the true symmetry to be monoclinic. An approximate estimate of the phase fractions in the two-phase samples was obtained from the relative intensities of the two sets of peaks and consideration of the predicted intensity ratios in Table I.

The lattice parameters at 300 K were determined from least-squares fits to the peak positions for each of the five samples, including the minority phases. If the nominal compositions of the samples are assumed to be correct, a fairly accurate estimate of the "true" compositions in the two-phase samples can be obtained from the estimated phase fractions and either the variation of the b parameter or the unit-cell volume, both of which are quite sensitive to small changes in x. The coexistence of two phases in crystals grown by the floating-zone technique can be attributed either

to differences in oxygen content or to fluctuations in Sr concentration in different parts of boule. In either case, x should be interpreted as the Mn^{4+} content or hole concentration, but only on a relative scale, since the actual oxygen stoichiometry of the as-grown sample is not known precisely. The lattice parameters and compositions derived from the above procedure are summarized in Table II and plotted as a function of x in Fig. 2. These results are qualitatively similar to those reported by Urushibara *et al*,[13] i.e., b decreases sharply, c increases fairly rapidly, and a decreases slowly with increasing x. It is interesting to note that there is a "crossover" at ~ 300 K for the a and b parameters at $x \approx 0.12$, signifying a change of sign in the basal-plane strain $s=2(a-b)/(a+b)$, corresponding to the disappearance of JT-type orbital ordering. The rapid change of b as a function of x is reflected in a tendency for the (020) peak to be somewhat broadened with respect to the others, as can be seen in Fig. 1 for $x=0.08$ and 0.10, for example. From the measured peak widths it is possible to estimate the compositional fluctuation Δx to be $0.001-0.002$ (FWHM) after correction for instrumental resolution.

Several sets of measurements were carried out as a function of temperature in order to map out the features of the structural transition. For nominal $x=0.08$, JT-type orbital ordering transitions occurred for the majority ($x=0.079$) and minority ($x=0.083$) phases at ~ 550 and ~ 530 K respectively, as inferred by a sharp downturn in the c parameter. No indication of any reentrant behavior was observed down to 20 K. The variation of the lattice parameters of the $x=0.079$ phase was qualitatively similar to that of $LaMnO_3$,[23] but the maximum strain s was much less, about -2.0 % vs. -3.7 %. Similar behavior was found for nominal $x=0.10$, in
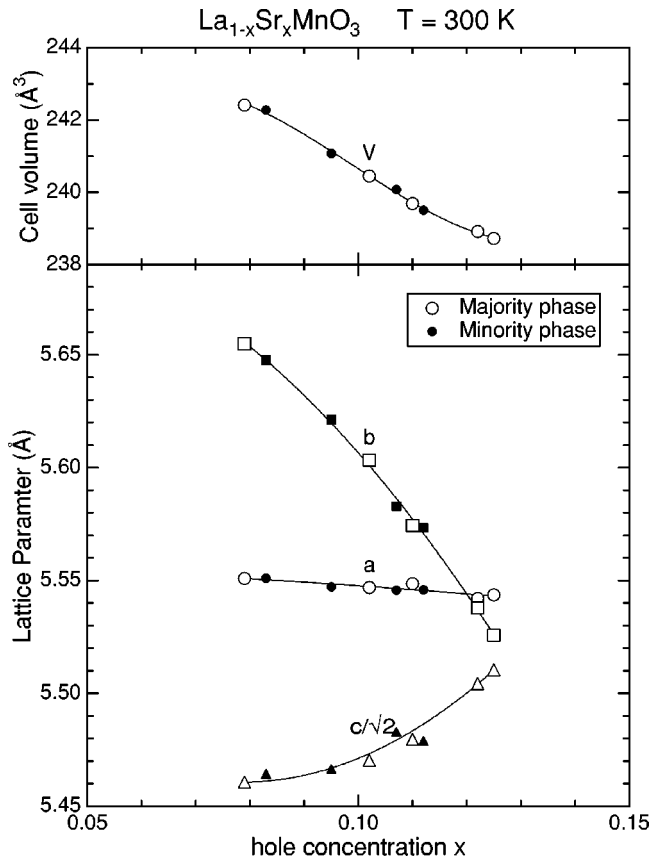
FIG. 2. The variation of lattice parameters for the five nominal compositions $x=0.08, 0.10, 0.11, 0.12$, and 0.125. The estimated ''x-ray'' compositions are derived from the unit-cell volumes based on the assumption that the actual overall composition is the nominal one.
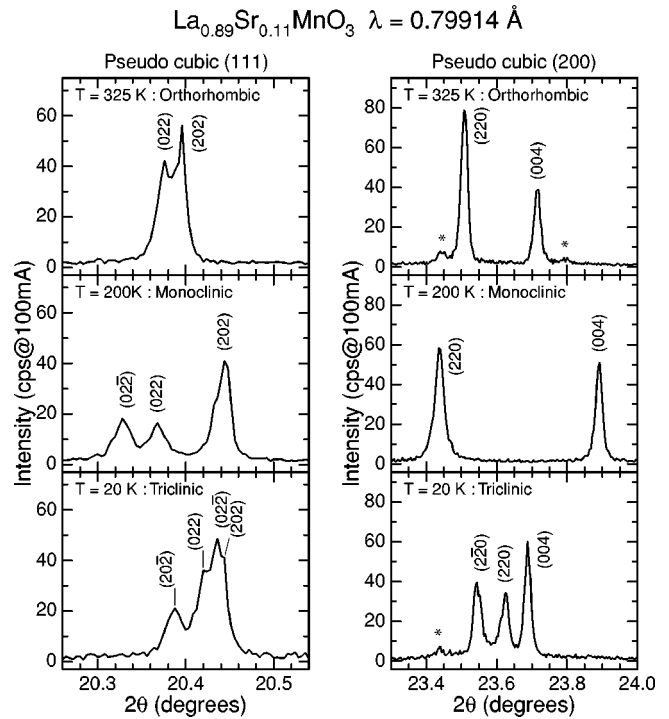

FIG. 3. Peak profiles of the pseudocubic (111) and (200) scans for the nominal composition $x=0.11$ at three temperatures, 325, 200, and 20 K, showing the evolution of the monoclinic and triclinic phases from the orthorhombic one.

which orbital ordering transitions were observed for the majority ($x=0.102$) and minority ($x=0.095$) phases at ~ 435 and ~ 455 K respectively, with values of s of -1.2% and -1.5% respectively at 20 K.

The behavior of the nominal $x=0.11$ sample was strikingly different, as illustrated by the scans of the pseudocubic (111) and (200) reflections shown in Fig. 3. At 325 K the peak splittings and intensity ratios confirm that the symmetry is orthorhombic (Table I). Between 320–105 K, the separation between the (220) and (004) peaks is approximately doubled, indicative of a cooperative JT ordered structure in the ab plane, and the (022) reflection is split into two roughly equal peaks, consistent with the monoclinic symmetry noted above. Quite remarkably, in addition to the abrupt change in lattice parameters previously reported[15,27–29,33] there is another distortion of the lattice below 105 K, clearly shown by the splitting of the (220) peak into two components with about the same intensity. Determination of the crystal symmetry is complicated by the large number of peaks and the high degree of overlap, but from a careful analysis of the peak positions and intensity ratios it is possible to conclude that the structure must be triclinic.

The variation of the lattice parameters and cell volume as a function of temperature is shown in Fig. 4. In order to differentiate between the a and b axes it was assumed that

reflections derived from the forbidden orthorhombic (201) reflection were also absent in the lower symmetry phases. These assignments are consistent with those reported in previous studies of $x=0.125$.[27,29] The orthorhombic-to-monoclinic phase transformation occurs over a coexistence range of about 5 K centered around 320 K (Fig. 4), at which point the two phases are present in roughly equal proportions, and there are small but abrupt changes in b, c, and α, respectively, indicative of a weakly first-order transition. In the coexistence region there are small changes in b and c for both phases which can be attributed to compositional fluctuations with $\Delta x \approx 0.002$. No hysteresis was observed within an experimental accuracy of ~ 1 K. Between $320-150$ K, there is a smooth increase in b and a, and a decrease in c indicative of a cooperative JT ordering, but the orthorhombic strain s is much less than in LaMnO$_3$. Below 150 K there is a slight downturn in b and upturn in c, followed by an abrupt change at ~ 105 K associated with the reentrant-type transition from monoclinic to triclinic symmetry. There is coexistence of the two phases over ~ 5 K, with a hysteresis on heating of $\sim 2-3$ K. The behavior shown in Fig. 4 is qualitatively similar to that previously reported for samples with $x=0.125$,[27,29] but the reentrant-type transition is much sharper in the present sample.

It is interesting to note the behavior of the very weak (220) peak from the minority phase with $=0.107$, which is well resolved at 325 K and below 105 K (as shown by asterisks in Fig. 3), and just discernible as a small shoulder in between. There is very little change in the position of this peak over the whole temperature range, and it is accordingly
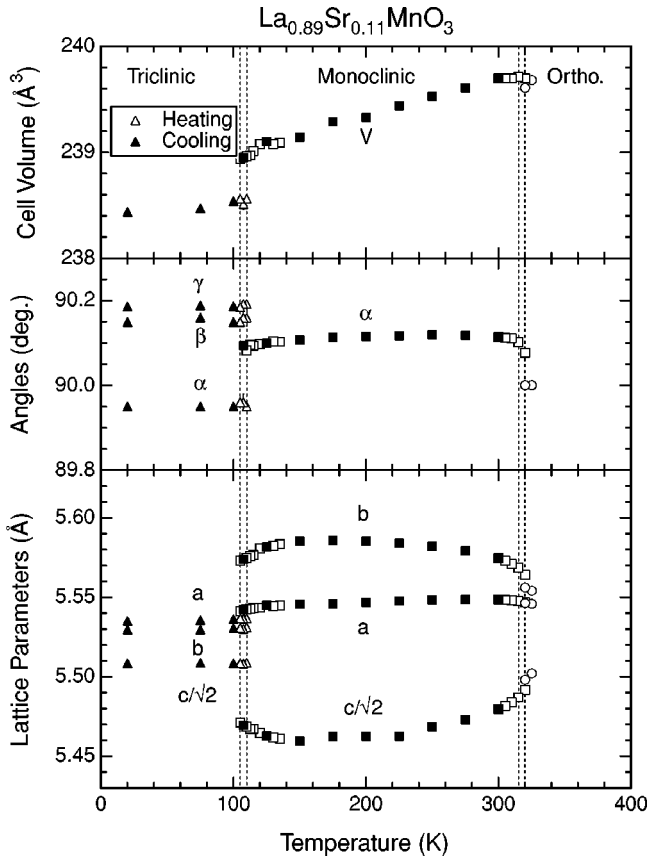
FIG. 4. Temperature dependence of (top) cell volume, (middle) angles, and (bottom) lattice parameters for the nominal composition $x=0.11$. The vertical dashed lines indicate the two-phase coexistence regions.

clear that this phase does not undergo a reetrant transition.

The sample with nominal $x=0.12$ shows well-resolved peaks from two phases at 300 K in the approximate ratio 3:1 (Fig. 1). In this case, the majority phase with estimated $x=0.122$ transforms to a JT-ordered monoclinic phase at ~ 295 K and undergoes a reentrant transition at ~ 140 K. The behavior of the minority phase, with an estimated $x=0.112$, is essentially the same as that of the $x=0.11$ sample, with transitions at ~ 320 and ~ 120 K.

Finally, the nominal $x=0.125$ sample, which appears to be single phase at 300 K, undergoes a first-order transition from orthorhombic to monoclinic at ~ 280 K with a narrow range of two-phase coexistence. Between $180-140$ K, there is a fairly gradual approach to a reentrant transition with a complex two-phase coexistence region, followed by an abrupt jump into a single-phase reentrant region. However, in this case the only indication of lower symmetry is a slight broadening of the (220) peak. The overall variation of the lattice parameters is in good agreement with the results of Pinsard *et al.*;[29] in particular, the unit-cell volumes at 300 K agree very closely, indicating that the hole concentrations x are the same within 0.002 of each other (see Fig. 2).

Values of the lattice parameters are listed in Table III for the majority phase in each of the five samples at selected temperatures in the different symmetry regions, designated by O^* (pseudocubic), O'_{JT} (JT-ordered orthorhombic), M_{JT}

(JT-ordered monoclinic), and T (triclinic). Also tabulated are the basal-plane strain s which is seen to be positive in the O^* and T regions, but negative in the O'_{JT} and M_{JT} regions. The assignment of triclinic symmetry to the $x=0.125$ sample at 75 K must be regarded as very tentative, since it relies mainly on the decomposition of the (220) profile into two peaks.

Based on the temperature dependence of the lattice parameters of both the majority and minority phases, it is possible to construct a revised structural phase diagram in this narrow region of composition, as illustrated in Fig. 5. This new phase diagram contains the essential features of the ones proposed by Kawano *et al.*[15] and Pinsard *et al.*;[29] in particular, the existence of a narrow ''reentrant'' region between $x \approx 0.11 - 0.13$ at low temperatures, associated with a transition from a JT-ordered phase to a less-distorted FMI phase. However, in striking contrast to the previous results, this region is structurally far more complex than hitherto supposed: it does not retain orthorhombic symmetry, but instead undergoes a sequence of transitions from orthorhombic-monoclinic-triclinic symmetry. Furthermore, the line separating the O'_{JT} and M_{JT} regions is extremely sharp, lying within a narrow region of hole concentration between $x=0.107 - 0.112$. In this region, there is also a distinct discontinuity between the rapidly-decreasing slope of the $T_{O*O'}$ and the more gradually decreasing slope of T_{O*M}. There is an indication of similar behavior in the data reported by Pinsard *et al.*,[29] although their $T_{O*O'}$ values are significantly lower than those determined here. This could be due to small differences in hole concentration, which for lower values of x is very sensitive to the final heat treatment and gas atmosphere.[25] In this context, we note that after heating one sample of $x=0.10$ to 550 K, the initial orthorhombic phase was not recovered on cooling, but instead a monoclinic phase. Inspection revealed that the capillary had not been properly sealed, from which we infer that some oxidation in air must have occurred even at this low temperature.

V. DISCUSSION

The experiments described above have given a clear description of the different types of structure in terms of crystal symmetry, but a detailed determination of the corresponding atomic shifts in the monoclinic and triclinic phases is a far more difficult challenge. Extended data sets were collected with the linear PSD in these regions from the $x=0.11$ sample in order to check for any weak superlattice peaks associated with the lowering of symmetry, but no extra peaks were observed at intensity levels of $\sim 0.1\%$ of those of the strong peaks. In a recent powder diffraction study of charge-ordering in $La_{0.5}Ca_{0.5}MnO_3$, several superlattice peaks were found at this intensity level,[37] but even if charge-ordering were to occur in the present samples one would anticipate that any additional peaks would be an order-of-magnitude weaker than for the latter compound due to the much smaller fraction of Mn^{4+} (1/8 vs 1/2) .

At this stage, we can only speculate about possible features of the structures which are consistent with the crystal symmetry and variation of the lattice parameters. In this con-

TABLE III. Lattice parameters of the majority phase in each of the five samples studied at selected tempreatures in the various temperature regions, designated as O^* (orthorhombic pseudocubic), O'_{JT} (JT-ordered orthorhombic), M_{JT} (JT-ordered monoclinic), and T (triclinic). The assignment of the a and b parameters in the M_{JT} and T regions is based on the assumption that the forbidden orthorhombic (201) reflection is also absent in the latter regions. s is the spontaneous basal plane strain defined as $2(a-b)/(a+b)$. The figures in parentheses represent the estimated standard deviation from the least-squares fits, referred to the least significant digit(s).

x	T(K)	a(Å)	b(Å)	c(Å)	s (%)	Phase
0.079	580	5.5675(6)	5.5496(6)	7.8560(9)	0.32	O^*
	20	5.5497(9)	5.6646(9)	7.6845(18)	-2.05	O'_{JT}
0.102	570	5.5678(5)	5.5344(4)	7.8387(7)	0.60	O^*
	20	5.5534(3)	5.6212(11)	7.7108(15)	-1.21	O'_{JT}
0.110	325	5.5459(2)	5.5542(2)	7.7811(2)	-0.15	O^*
	200	5.5468(2) $\alpha=90.115(4)$	5.5853(2)	7.7251(2)	-0.69	M_{JT}
	20	5.5353(5) $\alpha=89.95(1)$	5.5295(5) $\beta=90.15(1)$	7.7903(1) $\gamma=90.19(2)$	0.10	T
0.122	305	5.5425(5)	5.5346(5)	7.7857(4)	0.14	O^*
	175	5.5448(4) $\alpha=90.103(9)$	5.5690(4)	7.7243(3)	-0.44	M_{JT}
	65	5.5315(8) $\alpha=89.93(2)$	5.5196(8) $\beta=90.18(1)$	7.7893(1) $\gamma=90.09(1)$	0.22	T
0.125	300	5.5437(6)	5.5257(6)	7.7929(8)	0.33	O^*
	200	5.5455(2) $\alpha=90.134(2)$	5.5622(2)	7.7333(3)	-0.30	M_{JT}
	75	5.5338(1) $\alpha=89.96(1)$	5.5180(3) $\beta=90.14(1)$	7.7879(1) $\gamma=90.03(1)$	0.29	T

text, it is important to note that pulsed neutron studies in this composition range have shown that a local JT distortion is present even when the long-range crystallographic structure shows no such distortion.[38] What is quite clear from the present experiments is that there must be fundamental differences between the conventional JT-distorted structure in the orthorhombic O'_{JT} region, the JT-distorted structure in the monoclinic M_{JT} region, and the orbitally ordered triclinic structure in the FMI region. Although the behavior of the lattice parameters for $x=0.11$ in the M_{JT} region shown in Fig. 4 implies some kind of JT ordering in the ab plane, the fact that there is a monoclinic distortion and the results of the x-ray resonant scattering experiments both demonstrate that this cannot be the usual C-type antiferrodistortive arrangement found in the O'_{JT} region. The fairly abrupt crossover from the latter region to the M_{JT}/T region at $x \approx 0.1$, which may be related to the dimensional crossover in the magnetic excitations noted by Hirota et al.,[31] is further evidence of a quite different type of orbital order.

One possible structural picture is suggested by the nature of the monoclinic distortion, namely, that the unique axis is along [100] in the $Pbnm$ reference frame ($\alpha \neq 90°$), so that the b glide-plane symmetry element is preserved while the n and m elements are lost. The loss of the mirror plane would

be consistent with a change in JT order from C type to G type, in which there is antiferrodistortive coupling of MnO_6 octahedra along the c direction instead of parallel coupling. The corresponding space group $P2_1/c$ ($P2_1/b11$ in our nonstandard setting) would now permit reflections of the type $(h0l)$ with $h+l=$ odd, which are forbidden in space group $Pbnm$. Although no peaks of this type can be detected in the diffraction pattern, intensity calculations suggest that such peaks would be very weak as long as there is no change in the $a^- a^- c^+$ octahedral-tilt system characteristic of $Pbnm$ symmetry. Note that the G-type JT order in the M_{JT} region is consistent with the *disappearance* of the C-type orbital order as inferred from the missing of resonant x-ray scattering at $(00l)$ with $l=$ odd of $La_{0.88}Sr_{0.12}MnO_3$.[18] It is natural to assume that the G-type JT order is associated with the G-type orbital order, which should have resonant scattering at (101) and (011) instead of (001). Since (011) is structurally forbidden in $P2_1/b11$, while (101) is permitted, we would be able to see the resonant scattering if the G-type orbital order is realized in the M_{JT} region. This structure is also related to the ordered-polaron model for the FMI phase proposed in Fig. 4 of Yamada et al.,[17] to the extent that it corresponds to the configuration in the first and third layers along the doubled c axis, with the charge-ordered second and fourth
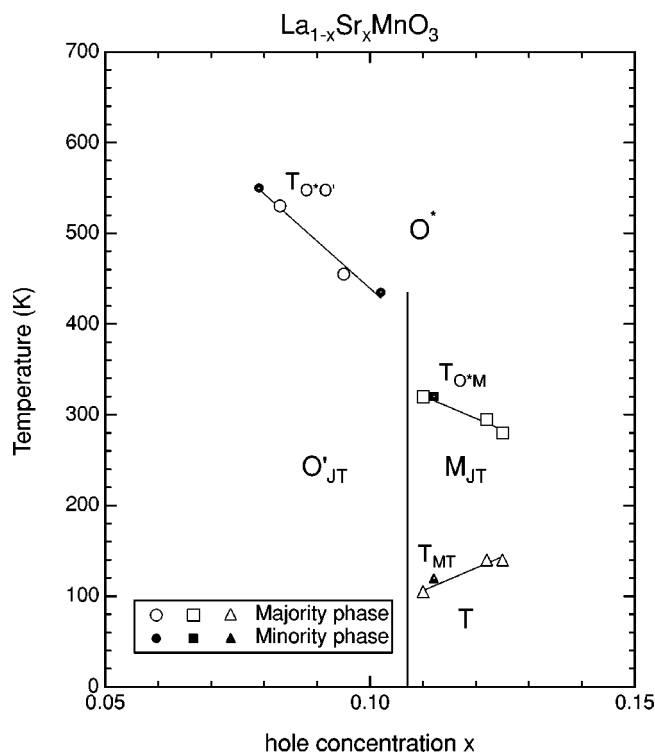
La$_{1-x}$Sr$_x$MnO$_3$

FIG. 5. A schematic plot of the phase diagram as a function of temperature for the ''x-ray'' compositions from the samples with nominal $x = 0.08, 0.10, 0.11, 0.12$, and 0.125.

ciated with orbital hybridization of the type proposed by Endoh *et al.*[18] Elucidation of this structure will certainly have to await a detailed single-crystal study.

After this paper was submitted, the results of a neutron diffraction reinvestigation of the low-temperature polaron-ordered structure of a crystal with $x = 0.1$ were published.[39] It was found that neither the previously proposed model in Ref. 17 nor a subsequent one proposed by Inami *et al.*[19] was consistent with the intensities of the observed satellite reflections. From a theoretical consideration of the interhole interactions a new type of polaron-ordered structure was proposed, involving ordering of two kinds of Mn atoms; in ''hole-deficit'' sites occupied solely by Mn^{3+} and in ''hole-excess'' sites occupied by ''Mn$^{3.25+}$.'' The orbital state of Mn$^{3.25+}$ is considered to be analogous to the state of a single Mn^{4+} in LaMnO$_3$ characterized as an ''anti-JT'' polaron,[40] and the most stable orbital configuration is found to be an orbital (polaron) wave along the c axis which results in a doubling of the lattice parameter in this direction. The lattice distortion can be visualized as the superposition of a normal JT mode and a breathing mode, alternating in a complex fashion along the c axis. The resulting structure is consistent with both the orbital order reported by Endoh *et al.*,[18] and also the observation of triclinic symmetry reported here, since this structure does not retain any of the symmetry planes and axes of the $Pbnm$ structure. However, it does not provide an intuitive explanation for the abrupt increase in the c lattice parameter, since the long Mn-O bond is still confined to the ab plane.

layers removed. Direct confirmation of such a structure from powder data would most likely require a combination of high-resolution and counting statistics that only an undulator beamline could provide, and may in fact require a very careful single-crystal study.

It is even more difficult to speculate about the nature of the triclinic structure. Clearly there is a drastic change in the type of orbital order in which the b glide plane is lost and presumably only the inversion center is retained. The doubling of the c axis observed in single-crystal studies must also be taken into account. The behavior of the lattice parameters implies a much more complex type of JT orbital order which is no longer confined to the ab plane, possibly asso-

*Present address: Lucent Technologies, P.I. Tres Cantos, s/n -Zona Oeste, 28760 Tres Cantos, Madrid, Spain.

†Present address: Institute for Materials Science, National Center for Scientific Research ''Demokritos,'' 15310 Agia Paraskevi, Athens, Greece.

‡Present address: CREST, Institute for Materials Research, Tohoku University, Katahira 2-1, Aoba-ku, Sendai 980-8577, Japan.

[1] S. Jin, T.H. Tiefel, M. McCormack, and R.A. Fatsnacht, Science **264**, 413 (1994).

[2] C. Zener, Phys. Rev. **82**, 403 (1951).

[3] P.W. Anderson and H. Hasegawa, Phys. Rev. **100**, 675 (1955).

[4] P.-G. de Gennes, Phys. Rev. **118**, 141 (1960).

[5] G.H. Jonker and J.H. Van Santen, Physica (Amsterdam) **16**, 337 (1950).

[6] J.H. Van Santen and G.H. Jonker, Physica (Amsterdam) **16**, 599 (1950).

[7] A.J. Millis, P.B. Littlewood, and B.I. Shraiman, Phys. Rev. Lett. **74**, 5144 (1995).

[8] H. Roder, J. Zhang, and A.R. Bishop, Phys. Rev. Lett. **76**, 1356 (1996).

[9] A.J. Millis, B.I. Shraiman, and R. Mueller, Phys. Rev. Lett. **77**, 175 (1996).

[10] S. Junoki, J. Hu, A.L. Malvezzi, A. Moreno, N. Furukawa, and E. Dagotto, Phys. Rev. Lett. **80**, 845 (1998).

[11] A. Moreno, S. Junoki, and E. Dagotto, Science **283**, 2034 (1999).

[12] Y. Murakami, J.P. Hill, D. Gibbs, M. Blume, I. Koyama, M. Tanaka, H. Kawata, T. Arima, Y. Tokura, K. Hirota, and Y. Endoh, Phys. Rev. Lett. **81**, 582 (1998).

[13] A. Urushibara, Y. Moritomo, T. Arima, A. Asamitsu, G. Kido, and Y. Tokura, Phys. Rev. B **51**, 14 103 (1995).

[14] H. Kawano, R. Kajimoto, M. Kubota, and H. Yoshizawa, Phys. Rev. B **53**, 2202 (1996).

[15] H. Kawano, R. Kajimoto, M. Kubota, and H. Yoshizawa, Phys. Rev. B **53**, R14 709 (1996).

[16] E.O. Wollan and W.C. Koehler, Phys. Rev. **100**, 545 (1955).

[17] Y. Yamada, O. Hino, S. Nohdo, R. Kanao, T. Inami, and S. Katano, Phys. Rev. Lett. **77**, 904 (1996).

[18] Y. Endoh, K. Hirota, S. Ishihara, S. Okamoto, Y. Murakami, A. Nishizawa, T. Fukuda, H. Kimura, H. Nojiri, K. Kaneko, and S. Maekawa, Phys. Rev. Lett. **82**, 4328 (1999).

[19] T. Inami, N. Ikeda, Y. Murakami, I. Koyama, Y. Wakabayashi, and Y. Yamada, Jpn. J. Appl. Phys., Suppl. **38-1**, 212 (1999).

[20] J.B.A.A. Elemans, B. van Laar, K.R. van der Veen, and B.O. Loopstra, J. Solid State Chem. **3**, 238 (1971).

[21] P. Norby, I.G. Krogh Andersen, E. Krogh Andersen, and N.H. Andersen, J. Solid State Chem. **119**, 191 (1995).

[22] Q. Huang, A. Santoro, J.W. Lynn, R.W. Erwin, J.A. Borchers, J.L. Peng, and R.L. Green, Phys. Rev. B **55**, 14 987 (1997).

[23] J. Rodriguez-Carvajal, M. Hennion, F. Moussa, A.H. Moudden, L. Pinsard, and A. Revcolevschi, Phys. Rev. B **57**, R3189 (1998).

[24] A.M. Glazer, Acta Crystallogr., Sect. B: Struct. Crystallogr. Cryst. Chem. **28**, 3384 (1972); A.M. Glazer, Acta Crystallogr., Sect. A: Cryst. Phys., Diffr., Theor. Gen. Crystallogr. **31**, 756 (1975).

[25] J.F. Mitchell, D.N. Argyriou, C.D. Potter, D.G. Hinks, J.D. Jorgensen, and S.D. Bader, Phys. Rev. B **54**, 6172 (1996).

[26] In fact, Rodriguez-Carvajal *et al.* note that this structure can be satisfactorily refined within *Pbnm* symmetry (Ref. 23).

[27] D.N. Argyriou, J.F. Mitchell, C.D. Potter, D.G. Hinks, J.D. Jorgensen, and S.D. Bader, Phys. Rev. Lett. **76**, 3826 (1996).

[28] L. Pinsard, J. Rodriguez-Carvajal, A.H. Moudden, A. Anane, A. Revcolevschi, and C. Dupas, Physica B **234-6**, 856 (1997).

[29] L. Pinsard, J. Rodriguez-Carvajal, and A. Revcolevschi, J. Alloys Compd. **262-3**, 152 (1997).

[30] T. Niemoller, M. von Zimmermann, S. Uhlenbruck, O. Friedt, B. Buchner, T. Frello, N.H. Anderson, P. Berthet, L. Pinsard, A.M. De Leon-Guevara, A. Revcolevschi, and J.R. Schneider, Eur. Phys. J. B **8**, 5 (1999).

[31] K. Hirota, K. Kaneko, A. Nishizawa, Y. Endoh, M.C. Martin, and G. Shirane, Physica B **237-8**, 36 (1997).

[32] R. Senis, V. Laukhin, B. Martinez, J. Fontcuberta, X. Obradors, A.A. Arsenov, and Y.M. Mukovskii, Phys. Rev. B **57**, 14 680 (1998).

[33] S. Uhlenbruck, R. Teipen, R. Klingeler, B. Buchner, O. Friedt, M. Hucker, H. Kierspel, T. Niemoller, L. Pinsard, A. Revcolevschi, and R. Gross, Phys. Rev. Lett. **82**, 185 (1999).

[34] H. Nojiri, K. Kaneko, M. Motokawa, K. Hirota, Y. Endoh, and K. Takahashi, Phys. Rev. B **60**, 4142 (1999).

[35] S. Ishihara, J. Inoue, and S. Maekawa, Phys. Rev. B **55**, 8280 (1997).

[36] L.W. Finger, D.E. Cox, and A.P. Jephcoat, J. Appl. Crystallogr. **27**, 892 (1994).

[37] P.G. Radaelli, D.E. Cox, M. Marezio, and S-W. Cheong, Phys. Rev. B **55**, 3015 (1997).

[38] D. Louca, T. Egami, E.L. Brosha, H. Röder, and A.R. Bishop, Phys. Rev. B **56**, R8475 (1997).

[39] Y. Yamada, J. Suzuki, K. Oikawa, S. Katano, and J.A. Fernandez-Baca, Phys. Rev. B **62**, 11 600 (2000).

[40] P.B. Allen and V. Perebeinos, Phys. Rev. B **60**, 10 747 (1999).